Controlled drug release from laser treated polymeric carrier

Litauszki K., Igriczné Kiserdei É., Pamlényi P., Szarka Gy., Kmetty Á., Kovács Zs.

Controlled drug release from laser treated polymeric carrier

Katalin Litauszki[1], Éva Kiserdei Igriczné[2], Krisztián Pamlényi[3], Györgyi Szarka[4], Ákos Kmetty[1,5*], Zsolt Kovács[6,7]

[1]Department of Polymer Engineering, Faculty of Mechanical Engineering, Budapest University of Technology and Economics, Műegyetem rkp. 3., H-1111 Budapest, Hungary
[2] Department of Organic Chemistry and Technology, Budapest University of Technology and Economics, Műegyetem rkp. 3., H-1111 Budapest, Hungary
[3]Institute of Pharmaceutical Technology and Regulatory Affairs, University of Szeged, Eötvös u. 6., H-6720 Szeged, Hungary
[4] Polymer Chemistry Research Group, Institute of Materials and Environmental Chemistry, Research Centre for Natural Sciences, Magyar Tudósok Körútja 2, H-1117 Budapest, Hungary
[5]MTA–BME Research Group for Composite Science and Technology, Műegyetem rkp. 3., H-1111 Budapest, Hungary
[6] Department of Experimental Physics, University of Szeged, Dóm tér 9., H-6720 Szeged, Hungary
[7] Wigner Research Centre for Physics, H-1121 Budapest, POB. 49, Hungary
*Correspondence: kmetty@pt.bme.hu; Tel.: +36 1-463-2004

Abstract: In this study, we present the effect of laser treatment on polymeric poly(lactic acid) drug carrier films. Our goal was to demonstrate the control of the drug-release kinetics of a polymeric carrier as a function of total absorbed laser energy. The controlled drug release kinetic was achieved by modifying the amorphous polymeric carrier's molecular weight via low energy density laser-exposure. According to gel permeation chromatography results, the decrease of molecular weight correlates with an increasing laser-shot number and shows a distinct saturation-like behavior. The dissolution test also suggests the presence of such dependency, as the rate and amount of caffeine released from the sample shows an increasing tendency up to 2000 laser shots. This fact proves that the laser treatment modifies the drug release. The approach presented here may complement other methods used for controlled drug release in various medical and pharmacological applications.

Keywords: controlled release, polymeric carrier, photodegradation, caffeine, laser

1. Introduction

The controlled reduction of the molecular weight of polymers has significant potential; an excellent example is pharmaceutical production, where polymers are widely used as raw materials [1]. Improving the bioavailability of active pharmaceutical ingredients (API) and controlled release have paramount importance and still an active research area [2]. Poly(lactic acid) (PLA) is a promising polymeric carrier [3,4]. Beneficial properties of PLA include biodegradability and release time in a wide range [5,6]. Use of a polymer carrier is advantageous because, depending on the properties of the polymer, the drug can be released in a controlled manner. The dissolution kinetics of the active ingredients is an essential feature of solid pharmaceutical preparations. One of the mechanisms of drug release is on the diffusion-induced concentration gradient. The concentration gradient is affected by the physical and chemical properties of the polymer. Examples of such chemical and physical properties, which have a significant effect on drug release, are the size and length of the molecular chains [7,8], and, if any, the number of crosslinks [1,9,10], crystallinity of the polymer [11,12], the processing technology used [13,14], the shape of the product [15], and surface roughness [16]. Currently, drug release from polymers is controlled in four ways: (1) by the type of the neat polymer material, (2) by the modification of the neat polymer with different additives [17-19], (3) by changing product geometry (e.g. microspheres, electrospun fibers [12,15,20-23]), (4) or the combination of methods (1), (2) and (3). Laser treatments are extensively researched and already used for welding [24], surface modification in medical applications [25] and to influence degradation of the polymer carrier [26]. Hsu et al. [27] reported that nanosecond ultraviolet laser irradiation (KrF excimer laser with a wavelength of 248 nm) accelerated the biodegradation of poly(L-lactic acid) films with a thickness of 20-25 μm. They used a homogenized laser beam for uniform surface treatment. The films were irradiated with a single pulse with a fluence of 1.80 J/cm^2 to 2.80 J/cm^2. The high-energy single pulse reduced crystallinity by melting the surface. Shibata et al. [28] used femtosecond laser irradiation on poly(lactic-co-glycolic acid) (PLGA) films with a thickness of 1 mm to demonstrate the difference in the biodegradation of PLGA films after femtosecond laser irradiation (400 nm 0.15 J/cm^2 and 15 000

pulses, and 800 nm 1.0 J/cm^2 and 15 000 pulses). They successfully determined that the degradation rate of a biodegradable polymer depends on the wavelength of the laser and irradiation with a 400 nm laser decreased the molecular weight of the PLGA on the surface layer following the laser treatment. However, they used focused femtosecond laser pulses. Therefore non-homogeneous initial degradation occurred locally. Although the short timescale of the interaction automatically provides the conditions for non-thermal (sub-picosecond) excitation, the scalability of this method is limited (with the exception of large dedicated user facilities) due to the relatively low energy yield of current table-top femtosecond laser systems.

In this present research, we used the laser method that we demonstrated earlier [29], which can successfully reduce the molecular weight of polymers such as biopolymer (PLA) films. Reducing the molecular weight of the biopolymer carrier allows finely controlled drug release, whereas in the case of excimer lasers with a microlens beam homogenizer or so-called unstable resonator arrangement uniform energy density can be achieved over an extensive surface. In the case of solid-state lasers, pulses with a mostly Gaussian beam profile can be converted to a flat, homogeneous profile with a compensating filter, but in many cases at the cost of significant energy loss. To prove this concept, we solution cast poly(lactic acid) films with caffeine as an active pharmaceutical ingredient, and applied our laser procedure to decrease the molecular weight of the drug-loaded PLA films. We irradiated the films with an excimer laser at a given wavelength using different energy dosages. The photodegraded films were characterized with differential scanning calorimetry (DSC), thermogravimetric analysis (TGA), attenuated total reflectance (ATR-FTIR), gel permeation chromatography (GPC) and a dissolution test to analyze the caffeine dissolution properties of the PLA samples with different molecular weights.

2. Materials and Methods

2.1. Materials

We used commercially available granulated extrusion grade poly(D-,L-lactide acid) 4060D (Ingeo Biopolymer, NatureWorks© LLC, USA) with 12.0 mol% D-lactide content. The weight average molecular weight of the PLA is 191 063 g/mol, the number average molecular weight is 116 894 g/mol, and the polydispersity index was measured as 1.63. It has a density of 1.24 g/cm^3; its glass transition temperature is 57 °C, crystalline content was measured as 0% by the authors previously [29,30]. We selected caffeine, in an anhydrous form (Ph. Eur.9., Molar Chemicals Kft, Hungary) as the model drug in powder form. Caffeine is a stimulant of the central nervous system and a diuretics drug. Chloroform (Molar Chemicals Kft., Hungary) was used as a solvent of PLA and caffeine.

2.2. Preparation of the film and specimens

For the experiment, we created a solution cast PLA reference film, and PLA films with 5 wt% caffeine content. All samples were 50 µm +/-10 µm thin. We prepared the solution from 3 g of PLA granules, 5 wt% of caffeine and 50 mL of chloroform, and stirred it for 45 minutes using a magnetic stirrer at room temperature for 45 minutes (24.4±1 °C, 60±2 % RH). Afterwards, the solution was cast in glass Petri dishes. 2 cm x 4 cm specimens were cut from the film for the laser treatment. The prepared films were stored protected from light in closed containers (24.4±1 °C, 60±2 % RH).

2.3. Excimer laser exposure

Up to 350 mJ/pulse UV radiation at 248 nm was provided by a Lambda Physik EMG 160 MSC, twin-tube unpolarized KrF excimer laser with a confocal unstable resonator configuration. This amplifier scheme rendered microlens homogenization unnecessary[29], due to higher coherence of the beam compared to the more conventional, stable flat-mirror arrangement. A notable benefit of this layout is a more efficient use of the total beam energy, as we are not limited by the aperture size of the microlens array.

The 1.5 cm x 3.5 cm initial beam was sent through a variable attenuator and a –f/7 diverging lens. When the beam reached the size of 7 cm x 4 cm, the center part of the beam was cut out by a 4 cm x 2 cm aperture. Before fixing the PLA samples to the backside of this aperture, pulse energy was monitored and set to 160 mJ (± 2 mJ), thus providing a constant 20 mJ/cm^2 fluence.

2.5. Testing methods

Absorbance measurement

We measured the absorbance of the film sample with a UV-2101 PC UV-VIS spectrophotometer (Shimadzu Corporation, Kyoto, Japan) in the 190–900 nm range and with an automatic sampling interval, using medium scan speed.

Differential scanning calorimetry (DSC)

We characterized the morphology of the resulted polymer matrix of the solution cast reference samples and the laser-treated samples using DSC with a Q2000 DSC device (TA Instruments, New Castle, DE, USA). The examined temperature range was 0–200°C. We used a heat-cool-heat scanning program with a heating and cooling rate of 5 °C/min. The weight of the samples was between 3 and 6 mg, and the tests were performed in protective nitrogen gas (50 mL/min). We used the first heating cycle to erase the thermal history of the samples. Using uniform cooling conditions, we cooled all samples down to 0 °C, therefore all of the samples had the same new thermal history. The degradation of the samples was characterized with the second heating up. We evaluated the glass transition temperature (T_g), the cold crystallization temperature (T_{cc}), the melt temperature (T_m), the degree of crystallinity after cold crystallization (χ_c, Equation (1)) and the degree of crystallinity before cold crystallization ($\chi_{c'}$ Equation (2)), where ΔH_m is the melting enthalpy and ΔH_{cc} is the cold crystallization enthalpy. The theoretical melting enthalpy of 100% crystalline PLA ($PLA_{100\%}$) is 93.1 J/g [31].

$$\chi_c = \frac{\Delta H_m}{PLA_{100\%}} * 100\ [\%], \quad (1)$$

$$\chi_{c'} = \frac{\Delta H_m - |\Delta H_{cc}|}{PLA_{100\%}} * 100\ [\%], \quad (2)$$

Thermogravimetric analysis (TGA)

Thermal degradation was characterized with a TGA Q500 device (TA Instruments, New Castle, DE, USA). The applied temperature range was 50-600°C and a nitrogen measuring atmosphere was used (60 mL/min). The heating rate was 10°C/min; the weight of the samples was between 3 and 6 mg. Thermal decomposition was characterized with the initial degradation as the temperature corresponding to 15% weight reduction ($T_{15\%}$ [°C]), the temperature corresponding to 60% weight reduction ($T_{60\%}$ [°C]), and the temperature of the maximum of the weight change rate (T_{dTGmax} [°C]).

Attenuated total reflectance Fourier-transform infrared spectroscopy (ATR-FTIR)

For ATR-FTIR measurements, we used a Tensor 37 transmission infrared spectrometer (Bruker, Billerica, MA, USA) and a Specac ATR IR head unit. The IR spectrum of the sample was recorded with a DTGS detector, 16-time sampling in the 4000 cm^{-1} to 600 cm^{-1} range.

Gel permeation chromatography (GPC)

We performed GPC on the samples to determinate the average molecular weight by number ($\bar{M}_n$), average molecular weight by weight ($\bar{M}_w$), peak molecular weight (M_p) and the degree of polydispersity (PD, where PD= $\bar{M}_w/\bar{M}_n$) of the samples. We used a tetrahydrofuran eluent, a Jetstream 2 plus thermostat, a Waters HPLC Pump 515 and Waters Styragel HR1, HR4 columns. We performed the analysis with an Agilent Infinity 1260 differential refractometer detector. Measurement temperature was 35°C, and the flow rate was 0.3 mL/min. We performed calibration based on narrow molecular weight polystyrene standards, with the PSS WinGPC software.

Dissolution test

A dissolution test was carried out on a 2 cm x 4 cm PLA film (containing 5 wt% caffeine) with a Titramax 101 vibration mixer (Heidolph, Germany). Mixing speed was 150 rpm at room temperature (25 °C). 40 mL distilled water was used as dissolution media. We measured 4 mL aliquots in 5, 10, 15, 30, 45, 60, 90, 120, 180, 240, 300, 360 minutes. The amount of aliquot was replaced after each sampling. The pipetted solution was tested because there is no absorption maximum for the polymer where the drug was measured. The aliquots were analyzed with a Genesys 10S UV-VIS (Thermo Fisher Scientific, Waltham, MA, USA) UV spectrophotometer at λ=273 nm.

3. Results and Discussion

3.1. Laser treatment

First, we measured the absorption spectra of the cast film (PLA_caff_ref) (Figure 1). Absorption of the PLA_caff_ref samples showed strong absorption under 300 nm, a characteristic convolution of the neat PLA and caffeine spectra. Due to our wavelength (248 nm), direct, non-thermal excitation of the PLA chains is expected without significant damage and/or generation of radicals in the caffeine molecules. To achieve an adequate degree of degradation of the polymer carrier, we chose 1000, 2000, 4000 and 6000 laser pulses with the previously presented laser arrangement (2.3). Designation of the samples is according to Table 1.

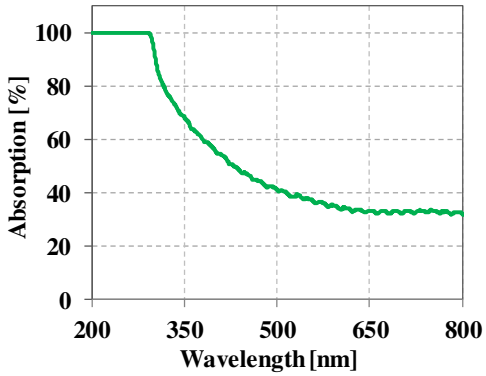

Figure 1 Absorption spectra of PLA_caff_ref film

Table 1. Samples prepared for different laser treatments

Sample name	Composition Polymer/drug		Treatment	Total dosage [mJ/cm^2]
PLA_ref	PLA	-	none	0
PLA_caff_ref	PLA	5wt% caffeine	none	0
PLA_caff_1000	PLA	5wt% caffeine	1000 laser pulses	20 000
PLA_caff_2000	PLA	5wt% caffeine	2000 laser pulses	40 000
PLA_caff_4000	PLA	5wt% caffeine	4000 laser pulses	80 000
PLA_caff_6000	PLA	5wt% caffeine	6000 laser pulses	120 000

3.2. Morphological properties of the films

We characterized the morphological properties of the samples using differential scanning calorimetry. We used the second heating up data of the thermogram to compare the morphology of the samples after deleting their thermal history [32]. Ingeo 4060D type of PLA has a D-lactide content of 12.0% [33], therefore, it has a low tendency to crystallize [34]. Our measurement results show (Table 2) that the presence of caffeine in the polymer film lowered the T_g. The reason for this is that small particles promote the mobilization of PLA molecules [35,36]. The T_g is 54 °C, but no cold crystallization and no crystalline fraction melting was registered (Figure 2). As a result of laser treatment, the tendency of PLA to crystallize did not increase because none of the laser-treated samples showed cold crystallization or a melting peak. Therefore, the crystalline fraction remained 0%. However, the T_g decreased as the number of laser pulses increased (Figure 3). The decreasing T_g is associated with expected photodegradation because lower molecular weight PLA has a lower T_g; this can be explained with the free volume theory, according to the literature [37,38].

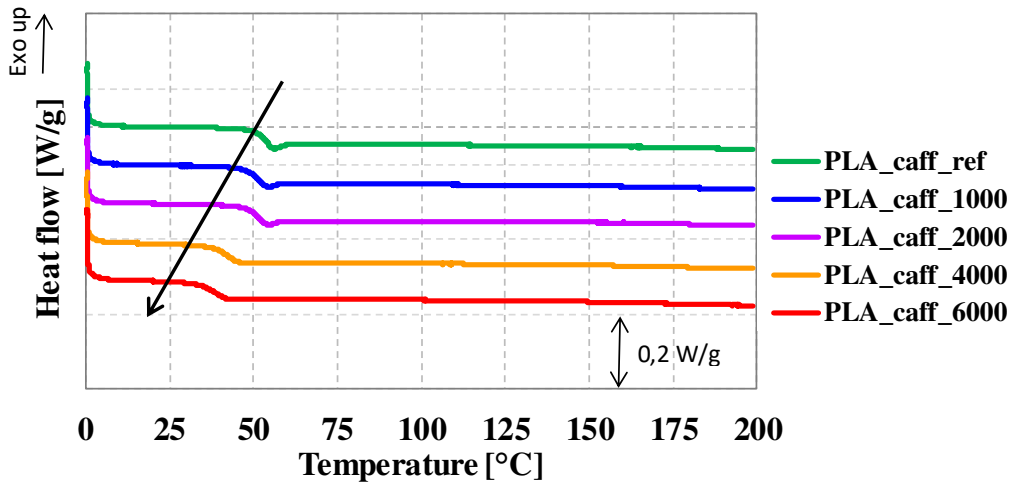

Figure 2. The DSC curves of the reference PLA and the laser-treated samples, 2nd heat-up, 5 °C/min (colored)

Table 2. Morphological characteristics of the reference PLAs and the laser-treated samples (5 °C/min)

	2nd heat-up cycle						
Sample name	T_g °C	T_{cc} °C	ΔH_{cc} J/g	T_m °C	ΔH_m J/g	X_c %	$X_{c'}$ %
PLA_ref	57	-	0	-	0	0.0	0.0
PLA_caff_ref	54	-	0	-	0	0.0	0.0
PLA_caff_1000	52	-	0	-	0	0.0	0.0
PLA_caff_2000	50	-	0	-	0	0.0	0.0
PLA_caff_4000	43	-	0	-	0	0.0	0.0
PLA_caff_6000	38	-	0	-	0	0.0	0.0

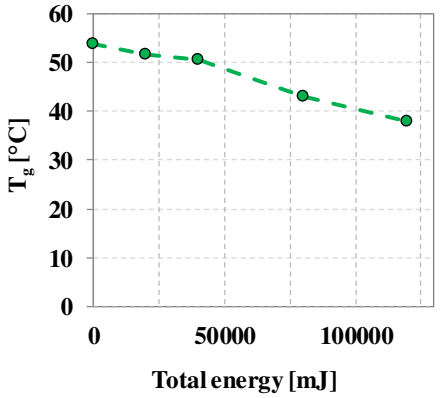

Figure 3. The glass transition temperature as a function of the number of laser pulses

3.3. Laser treatment effect on the thermal stability of the films

To prove the modification of the amorphous polymeric carrier's molecular weight via low energy density laser-exposure, we characterized the thermal stability of the samples. The thermal stability of polymers is classically quantified by initial degradation with the temperature corresponding to 5% weight reduction ($T_{5\%}$ [°C]), the temperature corresponding to 50% weight reduction ($T_{50\%}$ [°C]), and the temperature of the maximum of the weight change rate (T_{dTGmax} [°C]). In our case, we modified these values. We found that due to solvent casting, residual volatile content is released between 60-100 °C, and this is the first weight loss step. An additional, second weight loss was registered from 90 °C to 230 °C, which indicated the degradation of the caffeine content (Figure 4). The cast film sample that contains caffeine has a slightly higher thermal stability than the neat PLA film [39]. Using this information, we changed the evaluation of degradation characteristics. The initial degradation of the PLA with the temperature corresponding to 15% weight reduction ($T_{15\%}$ [°C]), the temperature corresponding to 60%

weight reduction ($T_{60\%}$ [°C]), and the temperature of the maximum of the weight change rate (T_{dTGmax} [°C]) remains the same (Table 3). Figure 5 shows the effect of laser treatment. The initial degradation temperature ($T_{15\%}$) of PLA after 1000 laser pulses is not different from that of PLA_caff_ref. However, as the number of laser pulses increase, $T_{15\%}$ decreases, and so does the energy absorbed by the polymer. The weight loss curves of samples treated with 1000 and 2000 laser pulses show lower degradation temperatures than the reference curve (Figure 5 a). However, the $T_{60\%}$ values of samples are only slightly different. Samples treated with 4000 and 6000 pulses have a significantly reduced $T_{60\%}$ (306 °C and 300 °C, respectively). This result indicates with great certainty that the molecular weight of the samples was successfully reduced. The dTG curve of the PLA_caff_6000 sample (Figure 5 b) has a bimodal characteristic; this is probably because the PLA_caff_6000 sample has a bimodal molecular weight distribution as well. We also investigated the thermal stability of the drug (Figure 6). According to the TGA results, caffeine was not degraded by laser treatment.

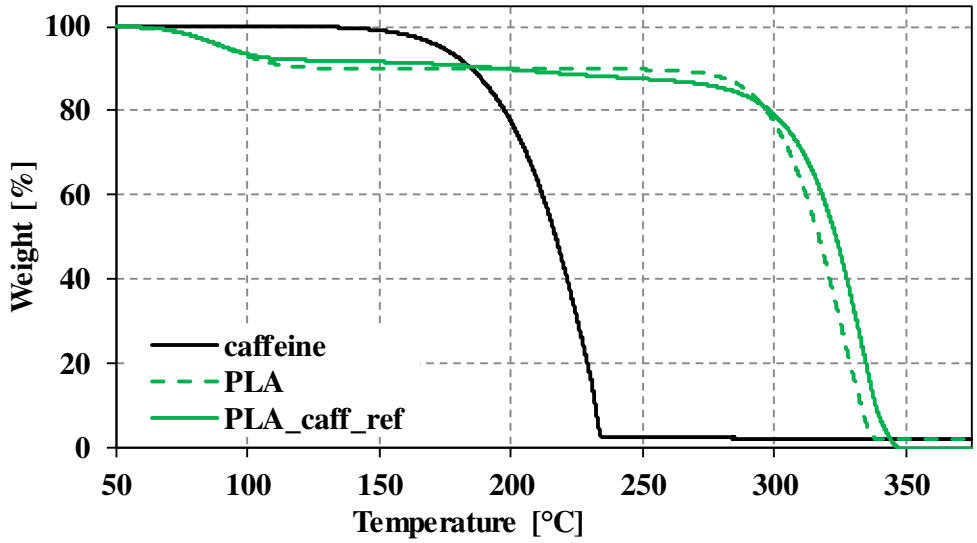

Figure 4. TGA results of caffeine, neat PLA and PLA with caffeine (10 °C/min) (colored)

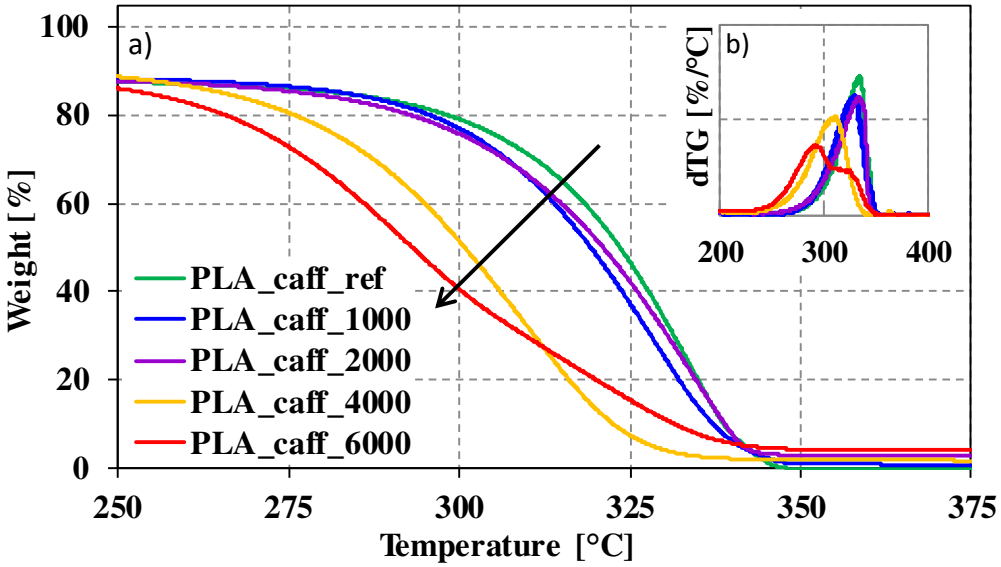

Figure 5. (a) TGA and (b) dTG results of the reference and the laser-treated samples (10 °C/min) (colored)

Table 3. Thermal decomposition characteristics of the reference and laser-treated samples (10 °C/min)

Sample	$T_{15\%}$ °C	$T_{60\%}$ °C	T_{dTGmax} °C
PLA_caff_ref	283	328	334
PLA_caff_1000	283	324	326
PLA_caff_2000	278	326	335
PLA_caff_4000	266	306	312
PLA_caff_6000	254	300	293

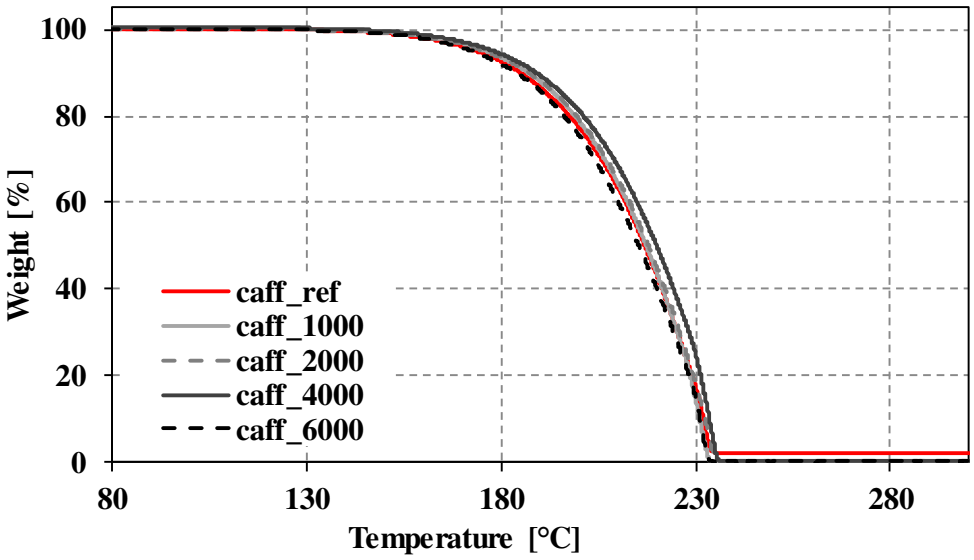

Figure 6 TGA results of non-laser treated and laser treated caffeine sample (10 °C/min)

3.4. Laser treatment effect on the molecular weight distribution of the films

To determine the chain scission of the polymer carrier due to the laser treatment, we determined the molecular weight distribution of the polymer using gel permeation chromatography. The molecular weight distributions are shown in Figure 7 and the evaluated $\bar{M}_w$, $\bar{M}_n$, $\bar{M}_p$ and PD values are presented in Table 4. As a result of 1000 laser pulses, $\bar{M}_w$ decreased significantly, by 72 400 g/mol, and polydispersity increased from 1.83 to 2.92. With a higher number of laser pulses, photodegradation went further and became more intensive. 2000 laser pulses caused $\bar{M}_w$ to decrease from 150 600 g/mol to 142 900 g/mol and polydispersity increased further to 4.09. Samples PLA_caff_4000 and PLA_caff_6000, suffered more photodegradation than PLA_caff_1000 and PLA_caff_2000, and the weight average molecular weight decreased from 142 900 g/mol to 34 200 and 46 000 g/mol respectively. We used the Chi-square test to evaluate whether there is any significant difference between PLA_caff_4000 and PLA_caff_6000 or not. The χ^2_{crit} value is higher than 233.9, the degree of freedom is 569 and 1-p=0.05. Our calculated χ^2 value is 8.9, which is lower than $\chi^2_{crit.}$ It means that the difference between the molecular weight distribution of sample PLA_caff_4000 (Observed) and PLA_caff_6000 (Expected) is not significant. This probably means that we reached a plateau in the degradation of the PLA polymeric carrier. In sum, the molecular weight distributions correlate well with the previously presented glass transition temperature decreases (DSC), the decreasing weight loss temperature and the bimodal nature of dTG (TGA).

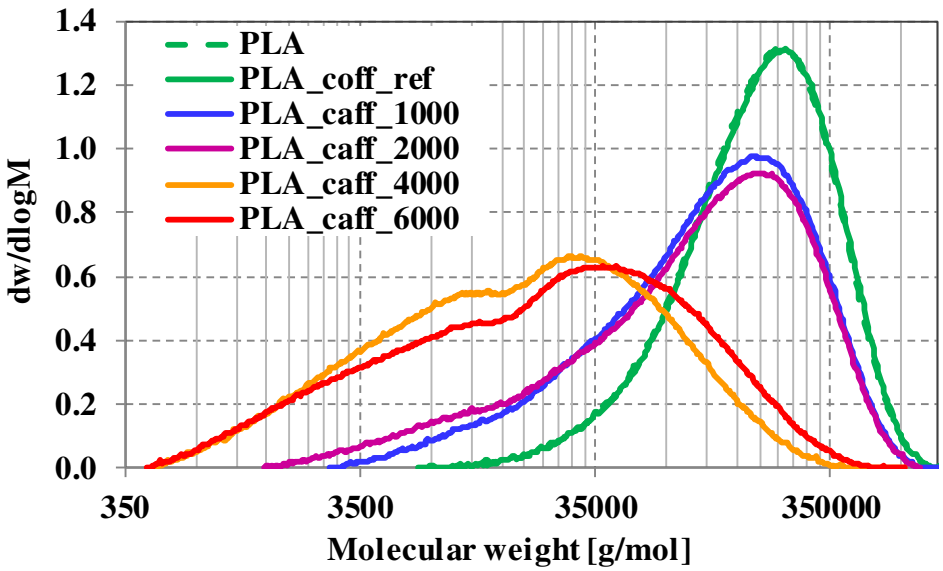

Figure 7. The molecular weight distribution of reference PLAs and the laser-treated samples (colored)

Table 4. The results of the GPC test of the reference PLA and the laser-treated samples

Sample name		Peak no.	M_p	$\bar{M}_n$	$\bar{M}_w$	PD
		-	g/mol	g/mol	g/mol	$\bar{M}_w$ / $\bar{M}_n$
caffeine	reference	1	90	90	91	1.01
PLA_ref	reference	1	208 000	122 000	209 000	1.71
PLA_caff_ref	reference	1	236 000	122 000	223 000	1.83
PLA_caff_1000	laser treated	1	167 000	51 600	150 600	2.92
PLA_caff_2000	laser treated	1	172 000	34 900	142 900	4.09
PLA_caff_4000	laser treated	2	27 700	6 800	34 200	5.03
PLA_caff_6000	laser treated	2	43 100	7 200	46 000	6.39

3.5. Fourier-transform infrared spectroscopy

We performed infrared spectroscopy to determine the changes in the chemical composition of the materials. The typical FTIR spectrum of caffeine has a characteristic spectrum with the main bands located between 1800 and 1500 cm^{-1}. The 1710, 1659, and 1554 cm^{-1} bands are the most intense. Intensity peaks at 1710 and 1695 cm^{-1} are due to the presence of two carbonyl groups. The peak at 1659 cm^{-1}, which is the strongest band in the middle IR, is the most interesting for the determination of the presence of caffeine [40]. The FTIR spectrum of PLA has intensity peaks: –CH– stretching modes (2997, 2946 cm^{-1} and 2877 cm^{-1}), a –C=O stretching region (strong 1759 cm^{-1}), $–CH_3–$ deformation (1456 cm^{-1}), –CH– deformation and asymmetric bands 1382, and 1365 cm^{-1}, –C–O– stretching of the ester group 1225 cm^{-1}, –C–O–C– asymmetric mode at 1090 cm^{-1}, and –C–C– stretch (871 cm^{-1}) [34]. Figure 8 a) shows the registered spectra of references (PLA, caffeine), the PLA_caff_ref and the laser-treated samples. In Figure 8 b) we focused on 1800-1500 cm^{-1}, where the most import bands are located, Major peaks at 1660 and 1705 cm^{-1} are related to the stretching vibration of carbonyl groups [40,41]. In contrast, neat PLA has no intensity peaks between 1725 and 1600 cm^{-1}. When caffeine was added to PLA (PLA_caff_ref), the above-mentioned two characteristic peaks appear. As a result of the laser treatment, the characteristic peaks disappeared because the free carbonyl groups ran out, due to the crosslinked structure and increasing interaction between caffeine and poly(lactic acid).

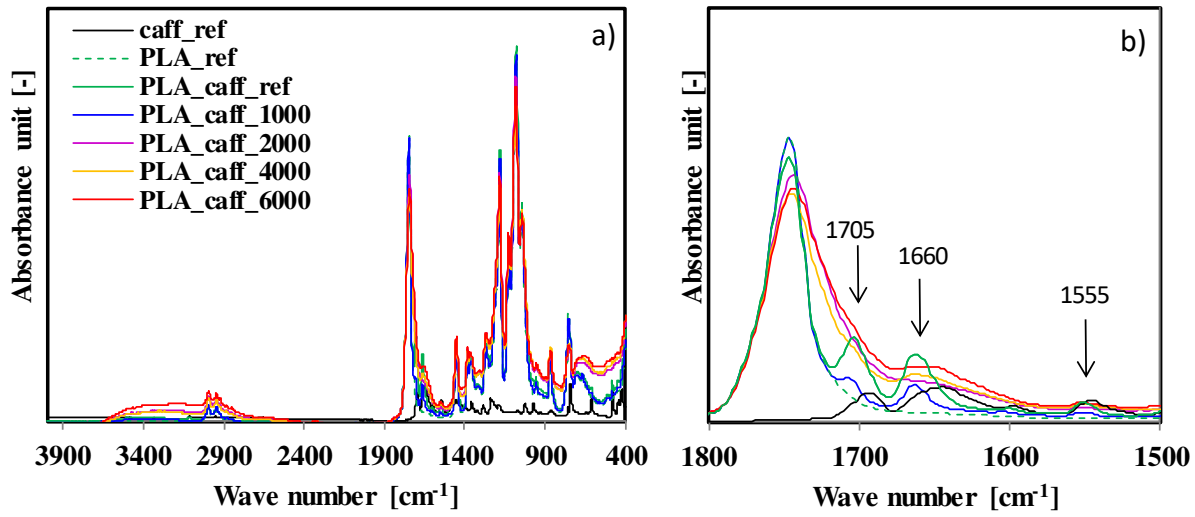

Figure 8. Infrared spectra of the caffeine, reference PLA films and laser-treated PLA films, (a) 4000-400 cm^{-1}, (b) 1800-1500 cm^{-1} (colored)

3.6. Dissolution test results

To determine the effect of controlled drug dissolution from the polymeric carrier via laser treatment, we carried out a dissolution test. Caffeine in free, dissolved form was detected in the dissolution measurement. The amount of released caffeine is presented as a function of time (Figure 9). Compared to the reference marked with red ($\bar{M}_w$ 223 000 g/mol), the amount of dissolved caffeine in the case of PLA_caff_1000 ($\bar{M}_w$ 150 600 g/mol) is already higher at 10 minutes, but after 60 minutes, it reaches the maximal released amount of caffeine. At the end, at 360 minutes, the amount of caffeine the reference released was 7.1%, while PLA_caff_1000 released nearly 20%. PLA_caff_2000, whose molecular weight was even lower ($\bar{M}_w$ 142 900 g/mol) than that of PLA_caff_1000, released even more caffeine (4.3%) in 10 minutes, and the amount of released caffeine is higher all along the measured range compared to PLA_caff_1000 and PLA_caff_ref. Total dissolution at 360 minutes is 27.8%. Our results indicate that as molecular weight decreases as a result of the increasing number of laser pulses, the rate and amount of caffeine released increases.

However, we found a deviation from the expected trend for the samples PLA_caff_4000 and PLA_caff_6000. The GPC test showed that molecular weight distributions shifted toward lower values because of the increasing interaction between the caffeine and polymer. On the positive side, the dissolution curves overlap, which supports that molecular weight distributions are very similar. However, the dissolution rate and amount of released caffeine are lower than for samples PLA_caff_1000 and 2000 and do not fit the trend. This may be because the concentration of released caffeine was determined from the intensity of the absorption peak measured at 273 nm. However, based on the FTIR results presented earlier, there is a presumed shift in the caffeine spectrum so that the concentration at 273 nm does not indicate the amount of caffeine actually released. The results show in the case of 1000 and 2000 laser pulses, dissolution follows the expected trend. In the case of 4000 and 6000 laser pulses, caffeine is not recommended because there was a change in its structure. These structural changes made UV detection difficult; for this reason, the curve runs lower in both cases. These findings are not limitations of the technology; it is merely the function of the active ingredient's material quality.

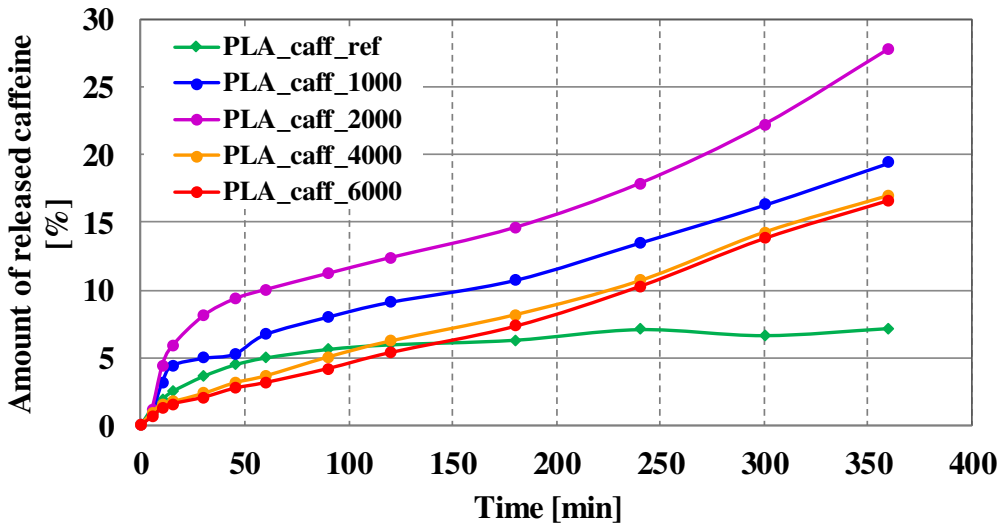

Figure 9. The dissolution test results of the reference PLA and the laser-treated samples (colored)

5. Conclusions

In this study, we presented the effect of a laser treatment of a polymeric drug carrier as a function of the irradiated energy to control the drug release of medicines. We successfully decreased the molecular weight of the polymeric carrier with an increasing number of laser pulses, as shown by DSC, TGA and GPC results. The DSC tests showed that the glass transition temperature decreased with an increasing number of laser pulses. The TGA results indicated that the initial degradation temperature ($T_{15\%}$) of PLA did not change after 1000 laser pulses compared to the reference PLA_caff_ref sample. A further increase in the number of laser pulses, however, caused $T_{15\%}$ to decrease. In the case of the PLA_caff_6000 sample, the dTG curve has a bimodal characteristic; this is due to the bimodal molecular weight distribution of the sample. The GPC results showed that an increase in the number of laser pulses caused increasing photodegradation, which resulted in a decrease of the molecular weight of PLA, up to 4000 laser pulses. The results indicate that with a decrease of the molecular weight caused by the increasing number of laser pulses, the rate and amount of caffeine released increases up to 2000 laser pulses. 2000 laser pulses is a limit of the chosen model drug. For other drugs, it is presumably possible to control the kinetics of drug release up to 4000 laser pulses in parallel with the molecular weight. The method presented for PLA can be used successfully for controlling of drug release for implants under the skin or long-release formulations for vaginal applications.

Funding:

This research was supported by the ÚNKP-19-3 New National Excellence Program of the Ministry for Innovation and Technology (ÚNKP-19-3-I-BME-261). The research reported in this paper is part of project no. BME-NVA-02, implemented with the support provided by the Ministry of Innovation and Technology of Hungary from the National Research, Development and Innovation Fund, financed under the TKP2021 funding scheme. The research reported in this paper and carried out at BME has been supported by the NRDI Fund (TKP2020 NC, Grant No. BME-NCS) based on the charter of bolster issued by the NRDI Office under the auspices of the Ministry for Innovation and Technology. The authors would like to acknowledge the European Social Fund EFOP-3.6.2-16-2017-00005 entitled by Ultrafast physical processes in atoms, molecules, nanostructures and biology structures grant, as it enabled us to use the laser facilities at University of Szeged. Á. Kmetty is thankful for the support of János Bolyai Research Scholarship of the Hungarian Academy of Sciences.

Credits:

Katalin Litauszki: Conceptualization, Methodology, Investigation, Validation, Formal analysis, Writing - Original Draft, Visualization, Supervision, Project administration. **Éva K. Igriczné**: Investigation, Validation, Writing - Review & Editing. **Krisztián Pamlényi**: Methodology, Validation,

Writing - Original Draft. **Györgyi Szarka**: Investigation, Validation, Writing - Review & Editing. **Ákos Kmetty**: Conceptualization, Supervision, Writing - Review & Editing**. Zsolt Kovács**: Conceptualization, Methodology, Writing - Original Draft

Acknowledgements: -

Data Availability: The raw/processed data required to reproduce these findings cannot be shared at this time as the data also forms part of an ongoing study.

References

1. Liechty WB, Kryscio DR, Slaughter BV, Peppas NA 2010. Polymers for drug delivery systems. Annual Review of Chemical and Biomolecular Engineering 1:149–173.
2. Jermain SV, Brough C, Williams RO 2018. Amorphous solid dispersions and nanocrystal technologies for poorly water-soluble drug delivery – An update. International Journal of Pharmaceutics 535(1-2):379–392.
3. Józó M, Cui L, Bocz K, Pukánszky B 2020. Processing induced segregation in PLA/TPS blends: Factors and consequences. Express Polymer Letters 14(8):768–779.
4. Zumaya ALV, Martynek D, Bautkinová T, Šoóš M, Ulbrich P, Raquez J-M, Dendisová M, Merna J, Vilčáková J, Kopecký D, Hassouna F 2020. Self-assembly of poly(L-lactide-co-glycolide) and magnetic nanoparticles into nanoclusters for controlled drug delivery. European Polymer Journal 133:109795.
5. J. S. Bergstroem, D. Hayman 2016. An overview of mechanical properties and material modeling of polylactide (PLA) for medical applications. Annals of Biomedical Engineering 44:330–340.
6. Lorenzo MLD, Androsch R. 2018. Industrial applications of poly(lactic acid). ed., Cham, Switzerland: Springer.
7. Wang T, Xue P, Wang A, Yin M, Han J, Tang S, Liang R 2019. Pore change during degradation of octreotide acetate-loaded PLGA microspheres: The effect of polymer blends. Eur J Pharm Sci 138:104990.
8. Koshari SHS, Shi X, Jiang L, Chang D, Rajagopal K, Lenhoff AM, Wagner NJ 2022. Design of PLGA-Based Drug Delivery Systems Using a Physically-Based Sustained Release Model. J Pharm Sci 111(2):345-357.
9. Moritera T, Ogura Y, Honda Y, Wada R, Hyon SH, Ikada Y 1991. Microspheres of biodegradable polymers as a drug-delivery system in the vitreous. Investigative Ophthalmology & Visual Science 32:1785-1790.
10. Karakurt I, Ozaltin K, Vargun E, Kucerova L, Suly P, Harea E, Minařík A, Štěpánková K, Lehocky M, Humpolícek P, Vesel A, Mozetic M 2021. Controlled release of enrofloxacin by vanillin-crosslinked chitosan-polyvinyl alcohol blends. Materials Science and Engineering: C 126.
11. Kimura H, Ogura Y, Moritera T, Honda Y, Tabata Y, Ikada Y 1994. In vitro phagocytosis of polylactide microspheres by retinal pigment epithelial cells and intracellular drug release. Current Eye Research 13:353-360.
12. S. Ahmed, S. Kanchi, G. Kumar. 2019. Handbook of Biopolymers: Advances and Multifaceted Applications. ed., Singapore: Pan Stanford Publishing Pte. Ltd.
13. Sousa JJ, Sousa A, Podczeck F, Newton JM 1996. Influence of process conditions on drug release from pellets. International Journal of Pharmaceutics 144:159-169
14. Gaurkhede SG, Osipitan OO, Dromgoole G, Spencer SA, Pasqua AJD, Deng J 2021. 3D Printing and Dissolution Testing of Novel Capsule Shells for Use in Delivering Acetaminophen. J Pharm Sci 110(12):3829-3837.
15. Feng X, Li J, Zhang X, Liu T, Ding J, Chen X, Ameli A 2019. Electrospun polymer micro/nanofibers as pharmaceutical repositories for healthcare. Journal of Controlled Release 302:19–41.
16. Kalosakas G, Martini D 2015. Drug release from slabs and the effects of surface roughness. International Journal of Pharmaceutics 496(2):291-298.
17. Chow WS, Ishak ZAM 2020. Smart polymer nanocomposites: A review. Express Polymer Letters 14(5):416–435.

18. Schuurmans CCL, Mihajlovic M, Hiemstra C, Ito K, Hennink WE, Vermonden T 2021. Hyaluronic acid and chondroitin sulfate (meth)acrylate-based hydrogels for tissue engineering: Synthesis, characteristics and pre-clinical evaluation. Biomaterials 268:120602.
19. Yuan X, Liu R, Zhang W, Song X, Xu L, Zhao Y, Shang L, Zhang J 2021. Preparation of carboxylmethylchitosan and alginate blend membrane for diffusion-controlled release of diclofenac diethylamine. Journal of Materials Science & Technology 63:210-215.
20. Bu LL, Yan J, Wang Z, Ruan H, Chen Q, Gunadhi V, Bell RB, Gu Z 2019. Advances in drug delivery for post-surgical cancer treatment. Biomaterials 219:119182.
21. Wu M, Liu W, Yao J, Shao Z, Chen X 2021. Silk microfibrous mats with long-lasting antimicrobial function. Journal of Materials Science & Technology 63:203-209.
22. Xie X, Chen Y, Wang X, Xu X, Shen Y, Khan AuR, Aldalbahi A, Fetz AE, Bowlin GL, El-Newehy M, Mo X 2020. Electrospinning nanofiber scaffolds for soft and hard tissue regeneration. Journal of Materials Science & Technology 59:243-261.
23. Soares RMD, Siqueira NM, Prabhakaram MP, Ramakrishna S 2018. Electrospinning and electrospray of bio-based and natural polymers for biomaterials development. Mater Sci Eng C Mater Biol Appl 92:969-982.
24. N. Pagano, G. Campana, M. Fiorini, R. Morelli 2017. Laser transmission welding of polylactide to aluminium thin films for applications in the food-packaging industry. Optics & Laser Technology 91:80-84.
25. Antonio R, B. MAL, Jesus dV, Rafael C, Juan P 2018. Laser surface texturing of polymers for biomedical applications. Frontiers in Physics 6:16.
26. J. Yun-Wan, Z. Xi, F. Teng, L. De-Fu, G. Yan, W. Xiu-Li, W. Yu-Zhong 2020. Synergy effect between quaternary phosphonium ionic liquid and ammonium polyphosphate toward flame retardant PLA with improved toughness. Composites Part B: Engineering 197.
27. Hsu S-T, Tan H, Yao YL 2012. Effect of excimer laser irradiation on crystallinity and chemical bonding of biodegradable polymer. Polymer Degradation and Stability 97:88-97.
28. Shibata A, Yada S, Terakawa M 2016. Biodegradability of poly(lactic-co-glycolic acid) after femtosecond laser irradiation. Scientific Reports 6:1-9.
29. Litauszki K, Kovács Z, Mészáros L, Kmetty Á 2019. Accelerated photodegradation of poly(lactic acid) with weathering test chamber and laser exposure – A comparative study. Polymer Testing 76:411-419.
30. Kmetty Á, Litauszki K 2020. Development of poly(lactide acid) foams with thermally expandable microspheres. Polymers 12:463.
31. Hajba S, Tábi T 2019. Cross effect of natural rubber and annealing on the properties of poly(lactic acid). Periodica Polytechnica Mechanical Engineering 63(4):270–277.
32. G.W. Ehrenstein, G. Riedel, P. Trawiel. 2004. Thermal analysis of plastics - Theory and practice. ed., Munich, Germany: Hanser Publishers.
33. Standau T, Zhao C, Castellón SM, Bonten C, Altstädt V 2019. Chemical modification and foam processing of polylactide (PLA). Polymers 11:306.
34. R. Auras, L.-T. Lim, S.E.M. Selke, H. Tsuji. 2011. Poly(Lactic Acid) Synthesis, Structures, Properties, Processing and Applications. ed., New Jersey: Wiley.
35. Ho M-P, Lau K-T, Wang H, Hui D 2015. Improvement on the properties of polylactic acid (PLA) using bamboo charcoal particles. Composites Part B: Engineering 81:14-25.
36. L. Mészáros, B. Gonda. NANOCON 2017, Brno, Czech Republic, EU, Oct 18th - 20th 2017 2018, pp 212-217.
37. H. Cai, V. Dave, R. A. Cross, McCarthy SP 1996. Effects of physical aging, crystallinity, and orientation on the enzymatic degradation of poly(lactic acid). Journal of Polymer Science: Part B: Polymer Physics 34:2701-2708.
38. K. Liao, D. Quan, Z. Lu 2002. Effects of physical aging on glass transition behavior of poly(DL-lactide). European Polymer Journal 38:157-162.

39. Kumara TSM, Rajinia N, Huafengb T, Rajuluc AV, Ayrilmisd N, Siengchin S 2019. Improved mechanical and thermal properties of spent coffee bean particulate reinforced poly(propylene carbonate) composites. Particulate Science and Technology 37(5):643–650.
40. Garrigues JM, Bouhsain Z, Garrigues S, Guardia Mdl 2000. Fourier transform infrared determination of caffeine in roasted coffee samples. Fresenius Journal of Analytical Chemistry 366:319–322.
41. M.M. Paradkar, J. Irudayaraj 2002. A Rapid FTIR Spectroscopic Method for Estimation of Caffeine in Soft Drinks and Total Methylxanthines in Tea and Coffee. Food Chemistry and Toxicology 67:2507-2511.